Available online at www.sciencedirect.com
ScienceDirect
Advances in Space Research 42 (2008) 1108–1119
ADVANCES IN SPACE RESEARCH (a COSPAR publication)
www.elsevier.com/locate/asr

Planetary protection implementation on Mars Reconnaissance Orbiter mission ☆

J. Barengoltz [a,*,1], J. Witte [b]

[a] Jet Propulsion Laboratory, California Institute of Technology, 4800 Oak Grove Drive, Pasadena, CA 91109, USA
[b] Lockheed Martin Space Systems Company, Littleton, CO 80125, USA

Received 31 October 2006; received in revised form 28 September 2007; accepted 3 October 2007

Abstract

In August 2005 NASA launched a large orbiting science observatory, the Mars Reconnaissance Orbiter (MRO), for what is scheduled to be a 5.4-year mission. High resolution imaging of the surface is a principal goal of the mission. One consequence of this goal however is the need for a low science orbit. Unfortunately this orbit fails the required 20-year orbit life set in NASA Planetary Protection (PP) requirements [NASA. Planetary protection provisions for robotic extraterrestrial missions, NASA procedural requirements NPR 8020.12C, NASA HQ, Washington, DC, April 2005.]. So rather than sacrifice the science goals of the mission by raising the science orbit, the MRO Project chose to be the first orbiter to pursue the bio-burden reduction approach.

Cleaning alone for a large orbiter like MRO is insufficient to achieve the bio-burden threshold requirement in NASA PP requirements. The burden requirement for an orbiter includes spores encapsulated in non-metallic materials and trapped in joints, as well as located on all internal and external surfaces (the *total* spore burden). Total burden estimates are dominated by the mated and encapsulated burden. The encapsulated burden cannot be cleaned. The total burden of a smaller orbiter (e.g., Mars Odyssey) likely could not have met the requirement by cleaning; for the large MRO it is clearly impossible. Of course, a system-level partial sterilization, with its attendant costs and system design issues, could have been employed. In the approach taken by the MRO Project, hardware which will burn up (completely vaporize or ablate) before reaching the surface or will at least attain high temperature (500 °C for 0.5 s or more) due to entry heating was exempt from burden accounting. Thus the bio-burden estimate was reduced. Lockheed Martin engineers developed a process to perform what is called breakup and burn-up (B&B) analysis.[2] The use of the B&B analysis to comply with the spore burden requirement is the main subject of this article. However, several components aboard the orbiter were predicted to fail the minimum time at temperature requirements (or could not conservatively be shown to meet the conditions). An implementation plan was generated to address the highest contributors to the bio-burden assessment that fail to meet the requirements. The spore burden for these components was estimated by direct and proxy burden assays, NASA PP specifications, and dry heat microbial reduction, as appropriate. Items on the orbiter that required rework during assembly were also individually assessed. MRO met the spore burden requirement based on the B&B analysis, the MRO Planetary Protection Implementation Plan, and verification by the NASA Planetary Protection Officer's (PPO) independent assays. The compliance was documented in the MRO PP Pre-Launch Report. MRO was approved for flight by the NASA PPO.

Keywords: Planetary protection; Mars Reconnaissance Orbiter; Mars; Breakup and burn-up analysis

1. Background

Mars Reconnaissance Orbiter (MRO) Project is a Mars orbiter mission. Per NPR 8020.12C (NASA, 2005), it is a Category III mission, which has been confirmed by the NASA PP Officer (PPO). The unique planetary protection requirement for a Category III Mars orbiter mission is that either:

☆ The work described was carried out jointly by the Jet Propulsion Laboratory, California Institute of Technology, and by Lockheed Martin Space Systems Company (LMSSC), Littleton, CO 80125, under a contract with the National Aeronautics and Space Administration.
* Corresponding author. Tel.: +1 8182488421.
E-mail address: jbarengoltz@earthlink.net (J. Barengoltz).
[1] Glendale, CA 91208, USA.
[2] Lockheed Martin Corporation.

0273-1177/$34.00 © 2007 COSPAR. Published by Elsevier Ltd. All rights reserved.
doi:10.1016/j.asr.2007.10.001

The (aggregated) probability of impact of Mars by any hardware (other than the launch vehicle) launched out of Earth orbit must be <0.01 for a period of 20 years after the launch date *and* <0.05 for the period from 20 to 50 years after the launch date; or

The total bioburden (surface, mated and encapsulated) of all hardware (other than the launch vehicle) that may impact Mars must not exceed 5×10^5 aerobic spores at launch.[3]

A separate requirement on the launch vehicle or any of its subsystems requires the probability of impact of Mars not to exceed 10^{-4}. In addition, the spacecraft must be assembled and maintained in clean rooms of class 100K or better. Finally, all analyses, process records, and supporting information that demonstrate compliance must be documented.

The science orbit for MRO precluded compliance with the orbital lifetime (probability of impact) requirement. The MRO Project decided to demonstrate compliance with the total bioburden requirements, with a significant modification, i.e., relief from the burden requirement referring to the value *at launch*. The burden requirement is specified *at launch* (NASA, 2005) because the value includes the possible reduction of the burden during a mission to Mars due to environmental effects (e.g., vacuum, solar ultraviolet, etc.) However, entry heating is an environment unique to (nominal) orbiter missions. Its effect has not been considered in the general list of mission environments. For example, in a nominal Mars lander mission, entry heating can only affect the burden on the external surface of the heat shield (and possibly the backshell) of the aeroshell and the burden of the cruise stage, if any.

NPR 8020.12C (NASA, 2005) specifies that any part reaching a temperature of 500 °C for 0.5 s or longer is considered sterile.[4] MRO demonstrated by an entry heating breakup and burn-up analysis that portions of the spacecraft reach this temperature and time upon entry to the Mars atmosphere, and are exempt from the bioburden accounting.[5] The rationale for the acceptance of this approach by the NASA PPO is that although the spore burden *at launch* is the controlling requirement, the spores delivered to Mars are the important metric. It is also important that the entry heating that was considered in the analysis is a minimum (i.e., an accidental direct entry as occurred for Mars Climate Orbiter would involve much more heating). Finally no contact with Mars without the entry heating is possible. There is neither an action by the Project nor a possible failure mode so that the orbiter could impact Mars without it. The precedents for such an exception are the Mars Pathfinder,[6] Mars Polar Lander and Mars Exploration Rover heat shields and cruise stages, which were also granted exemptions based on entry heating analyses and the PP specification for sterility.

2. General approach to compliance

The MRO spacecraft was assembled and maintained at class 100K, with the usual exceptions for environmental testing, where appropriate measures were taken to prevent contamination. The statistics of the trajectories of the upper stage of the launch vehicle for each day of the window were analyzed to demonstrate compliance with the launch vehicle requirement. However, the use of the B&B analysis to comply with the spore burden requirement is the main subject of this article.

The planetary protection equipment list (PPEL), an EXCEL spreadsheet based on the flight system equipment list, was used to calculate, track and document the MRO total spore estimate. This list for MRO comprised 115 individual flight hardware components. In addition, a separate detailed PPEL for HiRISE (a large optical telescope), represented by a single entry in the main PPEL, ran to 91 items itself.[7] For each item, the number of units, its general materials of construction, the area of external surfaces, the area of internal surfaces and the volume of non-metallic materials were determined and recorded. The MRO spore estimate began with calculations of the spores on the surfaces and encapsulated in the bulk of non-metallic materials. For this purpose, PP specifications of spore densities were employed (NASA, 2005). Since the PP specification for spore density on surfaces depends on contamination control, the clean room class (if any) for the assembly of each item was recorded. Next, these values were reduced explicitly for any PP approved credit for the manufacturing processes of the item (not specifically for PP).[8] Refined bioburden estimates based on any assays were then recorded. Next, the effect of PP bioburden reduction processes was applied. Finally, the results of the breakup and heating process, from the B&B analysis, were entered into the table.

This detailed approach provided insight in reviews of the overall total burden estimate to the sources of spores,

[3] Note that the *exposed* spore burden requirement for a lander (3×10^5 spores) applies only to external surfaces and to a subset of internal surfaces relatively directly connected to the exterior. This difference between the requirements for landers and orbiters reflects the expected conditions of the different spacecraft when in contact with Mars.

[4] PP parameter specification "Time–Temperature for Sterility".

[5] They were treated as having zero bioburden in the total spore burden estimate.

[6] Also the external surface of the MPF backshell was shown to be sufficiently heated to be exempt.

[7] The HiRISE PPEL was later done in detail because, as one item at the PP specification bioburden density (no clean room), for the stable entry case B&B HiRISE alone would violate the burden requirement. For convenience, the details necessary to estimate the burden for HiRISE for the stable entry case were documented in a separate (linked) PPEL. Therefore assays were performed which reduced the estimate before B&B analysis results were applied. See Sections 4.2 and 5.

[8] For example, printed circuit boards are heated long enough and to a high enough temperature in their manufacture to take credit for a reduction in the encapsulated spore burden (no humidity requirement for encapsulated burden).

the sensitivity of the results to certain proposed design or procedural changes, and the sensitivity to the results of the B&B analysis itself. It also permitted rapid, accurate revisions of the spore estimates for improved area and volume data and for changes in the conclusions of the B&B analysis. Moreover, the actual spore burden estimate at launch *without* the exemption of hardware sterilized by the entry heating per the B&B analysis is available through the PPEL. This value is very conservative because, for the hardware that was exempt by the B&B analysis, no assays were performed (the spore density specification was used[9]) and typically no dry heat microbial reduction was applied.

2.1. Assays

All MRO microbiological assays were performed per the NASA standard assay method (NASA, 1980). Typically, these assays were only performed for components that were not exempt by the B&B analysis. In some cases, proxies for the flight units were assayed.

2.2. Dry heat microbial reduction

All dry heat microbial reduction (DHMR) was performed per the applicable PP specifications for four orders of magnitude reduction (NASA, 2005). All orbiter multilayer insulation (MLI)[10] and cables (with the exception of a few instrument MLI and cables) were so treated. Per the implementation plan, other components that were not exempt by the B&B analysis and that could tolerate DHMR were also dry heat processed.

3. Description of breakup and burn-up analysis

The breakup and burn-up analysis comprises trajectory analysis, entry heating analysis, breakup analysis, thermal analysis and ablation analysis. An entry trajectory analysis provided velocity and position (altitude) as a function of time. A Mars atmosphere model provided density as a function of altitude so that the dynamic pressure and heat flux at the stagnation point (leading surface) could be calculated as a function of time. A practical aerothermal heating analysis, supplemented with correction factors to the heat flux distribution from a computational fluid dynamics (CFD) analysis, allowed the calculation of temperatures at surface locations. The temperatures and dynamic pressures were compared to the limits of the orbiter mechanical design and materials to determine when the orbiter would break into its modules. Each released module was characterized by the time after entry and altitude of its release and its velocity. A new trajectory analysis was then started for these modules. The subsequent trajectory analysis of the orbiter (main core or bus) was modified to reflect its altered aerodynamic properties as it shed modules. A few-node thermal analysis was applied to representative modules for the estimation of the temperature of their components and also possible release, validated by a detailed multi-node thermal model for two electronics modules. A simple thermal ablation model was used for all released modules and components. This practical approach was validated by the thermal analysis for the selected representative modules. A careful account of the temperatures the modules and components reached was maintained.

3.1. Orbital decay analysis

The breakup and burn-up analysis began with the orbital decay analysis from the science orbit for the initial conditions at atmospheric entry. Since entry heating rates are proportional to velocity (v) raised to the third power and dynamic pressure is proportional to v^2, the minimum entry speed is a crucial parameter. This minimum value corresponds to a final decayed orbit (due to atmospheric drag) just before the rapid loss of altitude corresponding to entry.[11] The apoapsis and periapsis of the final orbit, the altitude of the final orbital pass and the orbiter's orientation were also determined. This part of the analysis was conducted using the POHOPA trajectory code.[12] The long-term propagation of the orbit considered solar pressure, atmospheric density and gravity effects, including higher order terms of the Mars gravity field. The atmospheric model used was the same Marsgram-2000 utilized for MRO aerobraking design. For conservatism, the lightest vehicle mass was used (corresponding to maximum propellant consumption at the end of the nominal science mission), since entry heating is generally reduced for lighter objects.[13] Also the most conservative heating environment for the vehicle was assumed to be the largest drag areas, which correspond to the aerobraking configuration.[14]

3.2. Entry trajectory analysis

The actual entry phase was propagated using LMSSC's aeroshell design tool CLAAS.[15] It produces velocity and density/temperature profiles for individual elements of an entering spacecraft, which are inputs for the aerothermal heat prediction tools, as well as load profiles for mechani-

[9] Which by intent should exceed any value determined by assay.

[10] Commonly called thermal blankets.

[11] Note that other events that would lead to entry, such as a failure during cruise phase or during Mars orbit insertion, would have much higher velocity than orbital velocity. Thus this is the minimum dynamic force and heating case.

[12] LMSSC multipass aerodynamic version of JPL POHOP (ca. 1995), modified to incorporate logic for aerobraking spacecraft.

[13] This assumption was confirmed for a heavy vehicle, corresponding to the mass at the end of aerobraking.

[14] The combination of the minimum mass and the maximum area also minimizes the time required for orbital decay. However, since the entry would occur in less than 20 years, this factor is not of interest.

[15] LMSSC 3-Degree of Freedom Entry Trajectory Code. The code is proprietary, but public domain codes exist.

cal strength assessments. The atmospheric model and the gravity field used were the same as for the orbital decay part of the analysis. Two orientations were considered: a stable attitude based on the statics of the center of mass and the center of pressure (which presents the propulsion module or aft end to the flow); and a tumbling case. The latter case was added to the analysis for catastrophic failures such as a meteoroid strike; analysis demonstrated that a tumbling orbiter might not damp into the stable attitude quickly enough for the analysis of the stable entry case to be correct.[16] For conservatism, the maximum drag area (aerobraking configuration) was used again for the stable case. For the tumbling case, the average presented area was used. The comparison of the lightweight and heavy vehicle entries using the long-term propagation plus entry simulation codes demonstrated, as expected, that the lightweight vehicle had lower heating (by 8%). Therefore the lightweight case is the most benign and thus most conservative entry case.

3.3. Structural degradation of orbiter (breakup) analysis

The purpose of the breakup analysis was to predict when various parts of the orbiter would break off (and therefore at what altitude and velocity). Based on the entry trajectory analysis, this analysis began when the altitude was 114 km (which defined the zero of time for subsequent analysis). Breakup can be caused by a dynamic pressure caused by the atmosphere that exceeds structural capability or by a temperature due to entry heating that exceeds design and test limits (e.g., adhesive failure, composite deck failure and struts weakening), or both. The breakup analysis used the results of the CLAAS trajectory analysis for altitude, density, and velocity as a function of time. The distribution of the heat flux (and a correlation factor) and dynamic pressure at the stagnation point was determined by an aerothermal environment code, SHIV.[17] This code was applied with the usual simplifying tumbling assumption for the tumbling entry analysis and for the analysis of released tumbling components, to obtain the stagnation point heating on the effective geometry, such as a cylinder or sphere of similar characteristic dimension. There are several limitations to this approach. For the stable entry analysis, the effective geometry analysis does not apply for the bus while it continues in a stable orientation. In addition, this approach may not provide accurate results for convective heating, given that such heating is more strongly a local phenomenon. For the orbiter breakup analysis, local heating details of both the non-tumbling bus and the tumbling bus are needed. In the present work, computational fluid dynamics (CFD) simulations were strategically applied to address local heating of the non-tumbling bus and the tumbling bus and to address heating to components attached to the bus (also, to quantify the integrated effects of tumbling on component heating). Significant corrections (for convection effects) to the SHIV results, which (conservatively) lowered the heat flux distribution, were obtained by the CFD code LAURA.[18]

A thermal analysis was performed with SINDA[19] on an orbiter multi-node thermal model to predict the time and altitude of each component ejection into the flow based on the temperature of the deck to which the component was fastened. The melting of the potting compound that retains the fastener (inserts) and the failure of the three composite decks and three gussets (which comprise much of the structure and to which most of the modules are mounted) were the main causes of module release.[20] That release time became the initial starting point for a detailed trajectory and heating analysis on that component. Further ablation or heating analysis was then performed to determine the fate of each component. One additional feature of the thermal analysis was the determination of the starting temperature for each component when it was finally released from an orbiter deck. A separate breakup analysis was performed for the stable entry and the tumbling cases.

3.3.1. Stable entry case

In the stable entry case, the solar arrays (SA) and the high gain antenna (HGA) fold backward due to the dynamic pressures overwhelming the unpowered gimbals. The trajectory is then modeled for this modified configuration. The bus continues in a stable configuration somewhat farther. In order to obtain the heating distribution for the bus, CFD was used to determine the aerothermal environment correction factors. The stable bus was modeled as an axisymmetric equivalent solid (Fig. 1). A flow simulation was performed on that geometry at a given freestream condition. The distribution of heat flux over the bus was normalized to the propellant tank stagnation value. The environment was then determined by applying the normalized heat flux as a correction factor to the SHIV analysis results, with the propellant tank radius as the effective geometry.

The Aft Deck and all components mounted to it are exposed to the direct entry heating. The MLI on the Aft Deck is rapidly burned away, exposing the components inside of it to the heating. The Aft Deck loses its integrity early in the entry as its composite structure is heated to the

[16] However, LMSSC did demonstrate by analysis that tumbling due to reaction wheel angular momentum unloading would dampen out rapidly enough for the stable case to apply. So the tumbling case applies only to the unlikely case of a meteoroid strike.

[17] The SHIV (*Sh*ock *I*nduced *V*orticity) Code is a proprietary LMSSC code for a locally similar boundary layer solution. However, public domain codes for aeroheating that employ the Sutton and Graves heating model, with arbitrary mixture equilibrium chemistry, in the hypersonic Mach regime and the Fay–Riddell model for lower Mach numbers exist. Turbulence and thermal radiation effects, although within the SHIV capabilities, were conservatively neglected.

[18] LAURA is a Langley Research Center 3-dimensional TLNS (Thin Layer Navier Stokes) solver.

[19] A commercially available thermal response code.

[20] Typically due to the melting of the aluminum core.

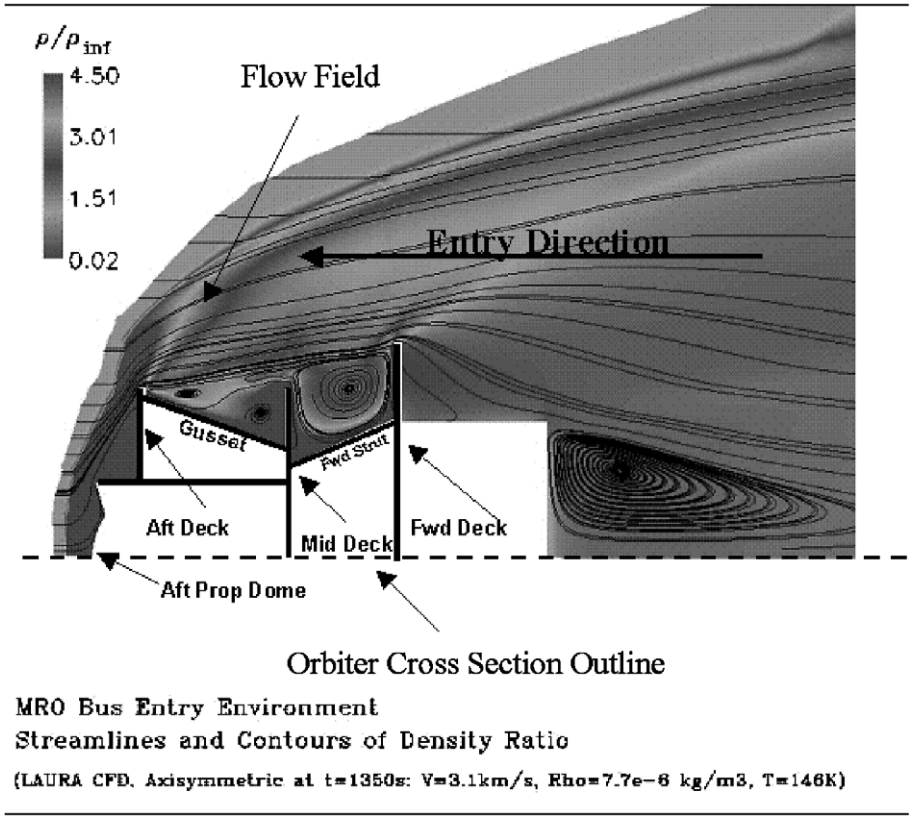

Fig. 1. CFD simulation results for the bus with contours of density ratio as well as flow streamlines. Flow is from left to right.

point where the aluminum honeycomb core melts. With the complete failure of the Aft Deck, a large number of avionics boxes are released into the flow including: the power distribution and drive unit (PDDU), the pyro initiation unit (PIU), reaction wheel assemblies (RWA), command & data handling subsystems (C&DH), the solid state recorder (SSR), main batteries, and helium tank.

The hypersonic flow coming around the vehicle warms the edges of the Forward Deck, in the "diving board" portions that hold the SAs and HGA. Next the SAs separate from the vehicle, followed by the HGA, due to the melting of the structural aluminum honeycomb core. Shortly afterwards, the four gusset panels that radiate outwards from the central propulsion tube core break up due to intense edge heating coupled with in-line flow along the panel flat surface. The loss of the gusset panels also causes the simultaneous separation of the Nadir Deck panel and, since it is also in similar thermal distress as the gussets, the separation of the avionics attached to it, the Compact Reconnaissance Imaging Spectrometer for Mars (CRISM) and the Mars Climate Sounder (MCS). The final major spacecraft event is the breakup of the Mid Deck, which releases the High Resolution Imaging Science Experiment (HiRISE) and the inertial measurement units (IMU) into the flow. What remains is the tank and core cylinder, although the core cylinder will probably ablate away with the gussets and Nadir Deck. All of these events occur in the time from 1040 to 1485 s after entry (except the Aft MLI, which is burned up by 500 s).

3.3.2. Tumbling entry case

The spacecraft configuration was modeled as an intact orbiter tumbling chaotically at an indeterminately high rate, but slow enough to retain the appendages before final entry descent. The trajectory analysis was allowed to proceed until the loads of the appendages exceeded the respective capabilities of the SA and HGA interfaces to the gimbal attach fittings.[21] The first appendages to be shed from the bus due to dynamic pressure are the SAs. The orbiter trajectory analysis was then modified for its new configuration without the SAs (and smaller average area). Shortly after that violent event the HGA follows suit, leaving the remaining bus and the rest of the intact components to descend together on their own trajectory (again modified for the loss of the HGA), as the SAs and HGA assume their own trajectories. Both of these events occur earlier (at higher altitude and velocity than for the stable entry case). Some parts of the multilayer insulation (MLI) also come off due to heating of its fastenings (but does not necessarily burn up) during this period. Thus the first set of major components the trajectories of which were followed further is the SAs, the HGA, some of the MLI and the bus (the more compact remainder).

[21] In the tumbling case, the SAs and the HGA are released due to fluctuating and direction-reversing dynamic pressure. For the tumbling case in general there is a greater potential to fail the structure through mechanical loading, while in the stable entry case the failure mechanism very often was thermal only.

In order to obtain the heating distribution for the bus, CFD was again used to determine the aerothermal environment correction factors. The bus was modeled as a box because once the orbiter's appendages are removed, the remaining orbiter attains the shape of a box in regards to how it appears to the entry flow. For chaotic tumbling, all sides were assumed to share heating equally (average heat flux). The CFD code was used to calculate the heat flux for each of (2) unique sides of a 2-dimensional box and for four angles of attack in one quadrant. The appropriate weight-averaged heat flux was calculated. Geometric equivalence was used to produce 13 angles of attack in the full circle in two dimensions. However, the tumbling added a complication to the heating analysis, the unknown tumbling rate. So, rather than analyze a large number of tumbling cases, a simplifying assumption was made to simulate the effect of tumbling by generating a pulsating heat flux on all sides of the bus and to simulate different tumbling rates by changing the pulse frequency. The results of this CFD analysis were then used to correct (for convective heating effects) the heat flux from SHIV.[22,23]

With the exception of the SAs and the HGA, two phenomena conspire to delay the structural release of components on the orbiter into the flow (compared to the stable entry case). First, the composite deck structure must achieve 250 °C before the potting material used for the fastener inserts softens to the point where centrifugal and aerodynamic forces pry the component away. Second, a view and blocking factor must be considered in the deck and component heating of a tumbling orbiter. The view of the heat flux by these components varies due to the tumbling. The influence of intervening components (''shadowing'') must also be treated. A ray-trace analysis was done to account for these factors before the detailed thermal analysis was performed.

As in the stable case, the trajectory analysis and the thermal analysis were performed to determine the time of release of further components from the bus. The breakup sequence for the tumbling orbiter as predicted by the continuing thermal analysis on the bus was very different than the stable entry case. In the stable entry scenario, components come off in groups (with the same initial conditions). The tumbling entry tends to have components ejected from the orbiter one at a time. This step-wise process required that each of forty-seven components be tracked and analyzed separately. All of the breakup events occur in the period from 855 to 1350 s after entry.

3.4. Thermal analysis of released modules and components

Thermal analysis of the released modules and components followed through to free components during the trajectory analysis for each piece. Both analyses are the same for the stable entry and tumbling entry cases because, with no real static equilibrium, the orbiter parts were assumed to tumble. Note that although the methods of these analyses for both the stable and tumbling cases were identical, the details and results of the analyses were unique, because the initial conditions for the various components were different. However, components that are released earlier in the breakup sequence for tumbling entry than for stable entry and were found to burn up or to achieve 500 °C were not analyzed again because the temperatures achieved must be higher for an earlier release (e.g., the SAs and the HGA).

The CFD code was again used to correct the correlation factor in SHIV for convection effects. The CFD results for a 2-dimensional box (Fig. 2) were augmented with CFD results for a thin 2-dimensional plate. The CFD code was used to calculate the heat flux for the one side of a 2-dimensional plate and for seven angles of attack in one quadrant. The appropriate weight-averaged heat flux was calculated. Geometric equivalence was used to produce 25 angles of attack in the full circle in two dimensions. The (previous) box solution was typically applied to all SHIV results for modules to obtain trajectory aerothermal environments (e.g., C&DH, CRISM, PDDU). The CFD values for the plate were applied to plate components (e.g., solar arrays, MLI blankets). The complication of an unknown tumbling rate was handled in the same manner as for the tumbling bus. With the SHIV heat flux as improved by CFD, the thermal analysis was conducted with two techniques, a thermal model and an ablation model. The heating and ablation and re-radiation analysis, after its validation, provided a simple screening to eliminate components that will certainly burn up into very small pieces from more detailed thermal analysis. For the other parts, engineering judgment was used to select worst case examples for groups of components (e.g., one structural panel to represent the others). These groupings were limited to items that enter the flow at similar times and are similar in makeup and size. The simplifying assumption was made that similar, but not identical, components would behave like the boxes that were analyzed in detail.

3.4.1. Thermal model

A simple few-node thermal model of selected representative modules was analyzed to determine the temperature as a function of time. The thermal model consisted of a few nodes (lumped masses) connected with conductors to form a network. The lumped masses and thermal conductances reflected the actual properties of the materials of construction. Heat was applied to the appropriate surfaces (nodes) which are in the flow and then re-radiated to the radiation sink temperature (boundary) which is assumed to be −58 °C. The thermal network was solved using the transient capabilities of SINDA.

The model for all of the structural ''plates'' (decks and gussets), also used during the breakup analysis, comprised three nodes (two facesheets and the aluminum core). The

[22] SHIV was also adjusted for the correct effective radius.

[23] For example, the results of the CFD correction to SHIV for the C&DH are shown in Fig. 2.

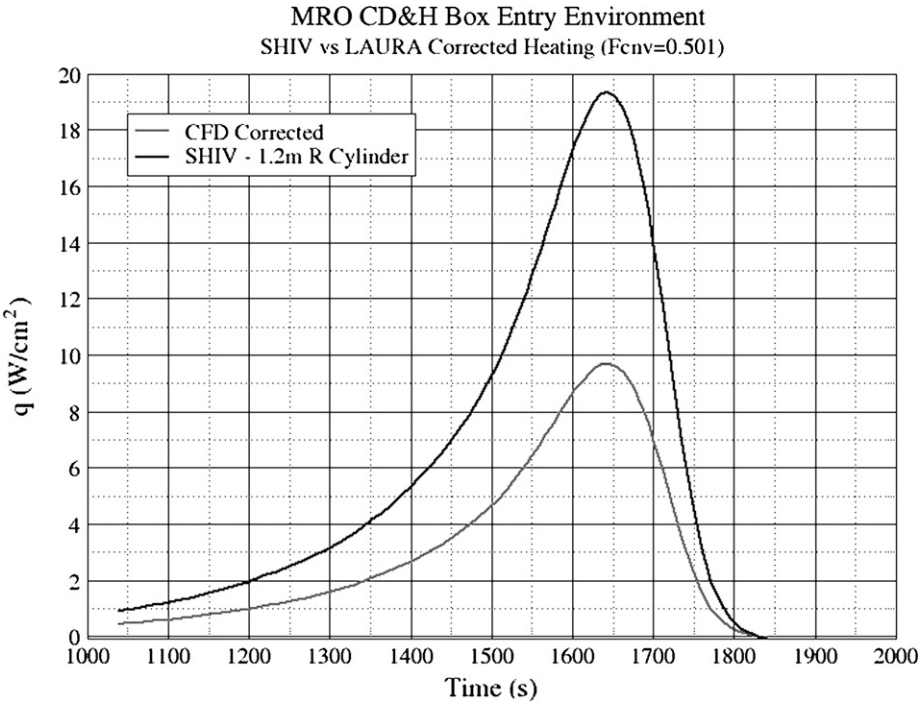

Fig. 2. SHIV vs. LAURA C&DH Entry Environment.

facesheet surface emittance was taken to be 0.3, a reasonable value for bare aluminum at elevated temperatures when the high emittance paint has ablated.[24] During the breakup analysis, heat flux from the trajectory analysis was not applied to these surfaces until the MLI that normally protects them had been shown conclusively to be removed. The model for the electronics modules was a 6-sided aluminum box with 2.54 mm (0.10 in.) thick walls. Each box wall was attached to the adjacent walls with a bolt conductance. The dimensions for each box were taken from the PPEL. The rest of the mass of the module (less the walls), i.e., the electronics, was lumped into a single node inside the box. The lumped mass was attached to only two sides of the box with a conductance that results in a 20 °C rise if the box is under normal operating power and thermal conditions. Heat fluxes from the trajectory analysis were then applied to each face of the box (module tumbling).[25] As the box walls reached 600 °C, the melting point of aluminum, the total heat flow, which was previously applied to the box walls, was applied to the lumped electronics node. A lumped mass approach is justified since once the box walls are removed, all internal surfaces will receive heating due to the gaps between electronic cards all of which are still attached to each other with the motherboard and other cables. This approach is conservative (underestimates the temperature), because the actual heating will occur over much more area due to the gaps between the Circuit Card Assemblies (CCAs). Thermal radiation from the lumped mass was estimated from only a surface area equal to the outside surfaces of the box. This is also conservative because the effective surface area for thermal radiation is less than this value. As a final conservative measure, no heat flux was applied until after the enclosure was completely ablated away. In fact, the edges and/or corners of the modules would most likely burn through beforehand, exposing the electronics assemblies to localized hot flow before the rest of the enclosure was consumed. This thermal analysis was performed for the C&DH, the SSR, the PIU, the PDDU, the battery (and its case), and CRISM. Analogous thermal analysis was conducted for the SA and HGA gimbals and the propulsion tank (after the core cylinder burns through and exposes it to the heating flow). Finally, detailed multi-node thermal models for the C&DH and PDDU in the tumbling entry case were constructed and analyzed with SINDA to obtain high fidelity temperatures for the CCAs (electronics).

3.4.2. Ablation model

The ablation model does not calculate the temperature of a module or component, but rather whether it burns up (by ablating away through heating up and melting, a function only of the energy it absorbs from the entry heating). The heat of ablation is defined as the sum of energy per unit mass required to heat an object to its melting temperature and the energy per unit mass required to melt it. This quantity was converted to the heat load required

[24] Also used in previous analyses by JPL for the cruise stage entry heating of the Mars Exploration Rover and Mars Pathfinder projects.

[25] As a sensitivity study to the tumbling assumption, an additional analysis was performed which assumed that only one side of the box was being heated at the total heat flux level of the tumbling C&DH case. The results showed that the CCAs reach a higher temperature than the tumbling box case.

(energy per unit surface area) for comparison with the heat flux results of the previously described analysis. The orientation of the parts relative to the flow that yielded the minimum temperature was employed and justified. A tumbling solution (for the parts) was also provided, as a source of a nominal temperature estimate.

The ablation analysis also considered thermal re-radiation. The model allowed for different emittances on one side from the other, or provided for a simple area averaging. The ablation analysis also considered the variation of the emittance of the leading surface as paints and coatings are removed.

The ablation model used for MRO included a layer analysis for the box housing and lumped parameter analysis for the contents of the box. For a general electronics box, the component consists of the outer housing, which is generally aluminum, and the inner electronics, which are a combination of copper, lead, glass, ceramic, and polyamide PCBs. The layer analysis of box ablation considered the outer housing first and allowed the calculation of how much heat (and therefore how much time) is required to burn through the housing of the box. The heat load is the product of the heat of ablation and the mass per unit area of the layer (e.g., typically the density of aluminum times the thickness of the box's skin). If the box is attached to a deck and one side is exposed to the flow, one side will burn through before the other sides.[26] Once the deck fails, the box will tumble. Then a new trajectory was used, and the heating was applied to all sides. Similarly, this method was also used to calculate the amount of heat required to burn through each layer of a composite panel. However, the box skin alone does not account for the total mass of aluminum housing because some mass is included in frame stringers or attachments. Consequently, a second calculation was done for total consumption of aluminum with the heat load corresponding to the remaining mass. Finally, the total heat required to consume the electronics was calculated for an amalgamation of materials with masses proportional to the C&DH electronics box construction, as a representative module. The surface area for the lumped mass of the electronics was estimated as the surface area of 1/2 of the volume of the original box, a thermal modeling technique.

This method of calculating heat of ablation and mass percentage of box electronics was used for all modules and components except the solar arrays, high gain antenna, HiRISE, CRISM, cables, reaction wheels, and gimbals. The gimbals and reaction wheels had metal internal details so they did not use the C&DH percentage of materials, but were otherwise analyzed similarly to the other boxes. All of the other exceptions are complex and were analyzed individually with a combination of the two methods.

[26] That is, this method was also applied for unreleased modules during the breakup analysis.

For the stable entry case, the ablation model was also employed in a sensitivity study for emittance of the surfaces and the time when the MLI was released. The most credible case (emittance 0.3 and MLI removal at 500 s) matched the structural analysis. The timing of MLI removal (10 s at most) did not have a large effect on the outcome of the ablation results.

3.4.3. Comparison of thermal model and ablation model analysis results

The results of the simple (few node) thermal models agreed reasonably with the results of the detailed multi-node thermal models run for the C&DH and the PDDU. The simple thermal model for the electronics modules was therefore validated. A correlation of the maximum temperatures for the electronics (CCAs) from both types of thermal models with the fraction of CCAs ablated as determined by the ablation model was constructed. The correlation shown in Fig. 3 is linear. At approximately 40% ablation and higher, all components are expected to achieve the 500 °C minimum temperature required 100% spore burden reduction. This temperature and ablation fraction correlation then became the basis for using the ablation analysis exclusively to determine the aero-heating temperature for the remaining components on the orbiter.

4. Results

4.1. Burn-up and breakup analysis

The MRO Project performed a conservative breakup and burn-up analysis which showed that much of the spacecraft is either ablated or reaches temperatures of at least 500 °C for 0.5 s (or more) during entry heating.

All external surfaces, including the external surfaces of modules and components that are released by the breakup, are ablated. Therefore the burden on these surfaces were discounted. This result eliminated the issue of recontamination after assays or dry heat microbial reduction, except where later rework (disassembly for repairs) was required.

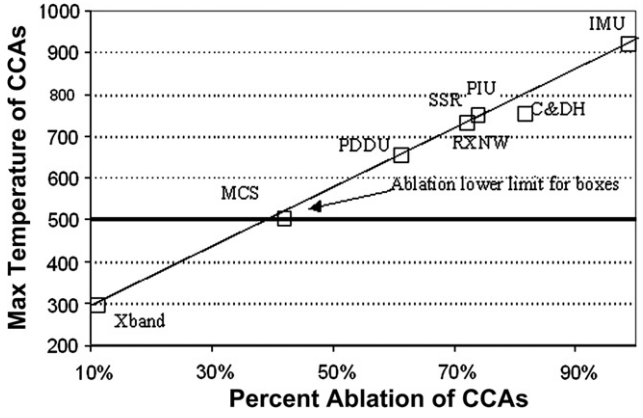

Fig. 3. Linear correlation of thermal and ablation analysis results.

In Table 1, the components of the orbiter that were not conclusively shown to attain 500 °C for at least 0.5 s are listed. This table is the source of the final estimates of the spores on MRO. The entry case (stable or tumbling or both) that led to the issue with the component is indicated. Also shown is the type of spore burden at issue (i.e., surface, mated or encapsulated). Finally, the method employed to establish an estimate for these accountable spores is noted. Note that the tumbling entry case was significantly worse for PP (many more components not exempt). A notable exception was the HiRISE, which was eliminated for the tumbling entry but not for the stable entry (only the shroud was eliminated for the stable entry case). Therefore a separate PPEL for HiRISE was constructed, and assays were performed (specifically on the optical bench). Thus HiRISE is noted as part assay, part PP specification in Table 1. Some of the components were dry heat microbially reduced. Other items were partially heated sufficiently for some reduction in their burden estimates (e.g., the various composite structure decks and gussets). In addition, hydrazine was assumed to be self-sterilizing and to sterilize surfaces that it contacts. This ''propellant effect'' is reflected in the entries for the propellant tank and the PCA and PIA Prop Components. Research supporting this conclusion has been completed (Schubert et al., xxxx). A detailed analysis of the release of the various sections of the MLI for the stable entry was conducted to show that it would be released in such a way as to burn up while its forward attachments held its trailing edges to the orbiter bus. However, it was not considered conclusive. This analysis could not be performed for the tumbling entry. Since released MLI might not be adequately heated *after* its release, the MLI could not be shown to be exempt. Many of the electronic modules, which were released early in the stable entry and then sufficiently heated, were released later in the tumbling entry. As a result, some of their electronics was not exempt. Cables were also problematical in either entry case. Finally, the gimbals were not exempt in the stable entry case. Gimbals, MLI and cables were all DHMR prior to installation onto the orbiter.

4.2. Assays

The results of the assays and the surface bio-burden densities derived are provided in Table 2. As expected, these

Table 1
Component/Subsystems that are not exempt from Spore Accounting

Item	Due to Stable S, Tumbling T, or both	Burden at Issue[a]			Burden basis
		I	M	E[b]	
Aft deck	T	x		x	Proxy assay
CPVs and sleeve clamps	T	x	x		Chem effect, proxy assay
Reaction wheel assemblies	T	x	x	x	Clean room assembly
Reaction wheel electronics (RWE)	T	x	x	x	Clean room assembly
He tank (He)	T	x	x	x	Clean, proxy assay, filtered
PDDU	T	x	x	x	Proxy assay, specification
PIU	T	x	x	x	Specification[c]
C & DH	T	x	x	x	Proxy assay, specification
SSR	T	x	x	x	Proxy assay, specification
All harness/cabling	S,T		x	x	Dry heat
Gussets	T	x		x	Proxy assay
Propellant tank	T	x			Clean & propellant effect,[d] filtered
PCA and PIA prop components	T	x			Clean & propellant effect
ONC instrument	T	x	x	x	Clean room assembly
MCS instrument	T	x	x	x	Clean room assembly
MCS electric motor	T	x	x	x	Clean room assembly
CRISM instrument OSU	T	x	x	x	Clean room assembly
CRISM electrical GME	T	x	x	x	Clean room assembly
Electra transceivers	T	x	x	x	Clean room assembly
Mid deck	T	x		x	Proxy assay
CTX instrument	T	x	x	x	Clean room assembly
SDST	T	x	x	x	Clean room assembly
IMU	T	x	x	x	Specification
Star trackers	T	x	x	x	Clean room assembly
HiRISE instrument	S	x	x	x	Assay, specification
HGA gimbal/support	S	x	x	x	Dry heat
Solar array gimbal/support	S	x	x	x	Dry heat
All MLI	S,T	x		x	Dry heat

[a] **I** is burden on internal surface area, **M** is burden on mated surface area, and **E** is burden encapsulated non-metallic volume. All external surfaces are exempted by B&B analysis. (See text.)
[b] Only **dry heat** affects (reduces) encapsulated burden.
[c] *Specification* refers to NPR 8020.12C (worst case uncontrolled manufacturing burden specifications). Unless otherwise noted these values were used.
[d] Hydrazine was assumed to be self-sterilizing and to sterilize surfaces which it contacted. (See text.)

Table 2
MRO assay results

Hardware item	Internal spores or density (m^{-2})	Purpose of assay
HiRISE optical bench	$<300\ m^{-2}$	Not exempt by B&B
Deck structure honeycomb interior	$41\ m^{-2}$	Part of decks not exempt by B&B Proxy assay of trim pieces
MRO battery CPV exterior and sleeve clamp i/f surfaces	78 per CPV	Not exempt by B&B
MRO battery sleeve mounting (to baseplate) surface	33 per CPV	Not exempt by B&B
LMSSC EMF facility work surfaces, board storage and proxy boards	$3000\ m^{-2}$	To establish a realistic density on C& DH, PDDU and other LMSSC electronics boxes interior
Helium tank primed surface thin film	1000, $2000\ m^{-2}$	To establish a realistic density on the tank internal surfaces (proxy tank)
CRISM MLI	2300	Not DHMR, proxy assay trim pieces
PDDU SASM (Backplane)	$980\ m^{-2}$ $510\ m^{-2}$	Rework (flight boards)
Gimbals	180	Rework without (a 3rd) DHMR
HiRISE FPA MLI	250	Not DHMR Proxy assay flight spare interior

values were smaller than the applicable (upper limit) PP specifications (NASA, 2005). The assay results for the HiRISE optical bench were particularly important for PP compliance in the stable entry case.

4.3. Rework and waivers

As planned, all hardware for which any assembly cleanroom credit had been taken was reworked in equivalent cleanrooms or better. For hardware that had undergone DHMR, the intent was to repeat the dry heat process.[27] The approach to waivers included estimates of the spores according to surface areas and non-metallic volume and PP specifications (NASA, 2005) (including cleanrooms) and a comparison with the remaining spore budget margin. In some cases assays were performed to lower the estimate.[28] New hardware was treated as though it was in Table 1, because the B&B analysis had not been shown to sterilize it.[29] Here again, estimates were made of its spore burden. Assays were performed where appropriate. Some new hardware was then DHMR. However, some new hardware created the concern of shielding pre-existing components and *possibly* invalidating part of the B&B analysis findings. These rare cases were reviewed carefully. The net effect of these changes was a modest increase of 1.8×10^4 spores, reflected in the final estimate.

5. Conclusions

MRO successfully met the requirement that the total bioburden at launch (surface, mated and encapsulated) of the part of the flight system that will contact Mars (i.e., the orbiter) shall not exceed 5×10^5 spores. The estimated "3 sigma" value was 4.4×10^5 spores for MRO. (This value corresponds to the tumbling entry case, which dominated. The value for the stable entry case was only 2.9×10^5 spores.) The sources of the spores that were not completely eliminated by the B&B analysis and their conservative number, adjusted for reduction by the B&B analysis as applicable, are indicated in Tables 3 and 4 for the tumbling and stable entry cases, respectively.[30] Note that HiRISE alone represents almost the entire estimate for the stable entry case. (HiRISE completely burns up in the tumbling case.) The extra detail in the HiRISE PPEL allowed the results of an exhaustive set of assays to be incorporated in the estimate for the stable entry case. This was essential for the demonstration of PP compliance.

As discussed throughout the description of the analysis to estimate the spore burden for MRO, an attempt was made to be conservative (overestimate the burden) at all times. The use of the term "conservative" in the B&B analysis means that when there was a choice of variables under consideration, they were generally chosen to maximize the opportunity for hardware survival to the surface. However, with only a few exceptions, the margins cannot be estimated. The burden estimates derived from the assay results are the only true three sigma values. The typical standard deviation of the burden density is about one third of the mean. Thus the burden estimates used may be twice the

[27] The only exception was the gimbals, which after a 2nd DHMR upon a 1st rework, were assayed during the last re-assembly following a 2nd rework (a 3rd DHMR was waived due to concern for the hardware).
[28] This included CRISM pigtail cables and MLI, HiRISE FPA MLI, and some MARCI cables, which were not DHMR.
[29] These items were: C&DH and AMCS filter boxes, SHARAD plume shield, and cable RF shielding.
[30] The percentages have not been updated for the small additional number of spores from rework and waivers, a minor correction.

Table 3
MRO bioburden estimates for top 15 hardware items not exempt by B&B analysis (tumbling case)

Item description by subsystem	B&B Adjusted Bioburden	% Total requirement
SSR	8.74E+04	17.5
PIU	7.26E+04	14.5
PDDU	5.91E+04	11.8
C&DH	4.92E+04	9.8
CRISM OSU instrument	3.11E+04	6.2
Reaction wheel electric boxes (RWE)	2.75E+04	5.5
Electra transceivers	2.47E+04	4.9
Gussets	1.29E+04	2.6
Helium tank	1.02E+04	2.0
Mid deck	7.43E+03	1.5
IMU	7.38E+03	1.5
Star trackers	6.13E+03	1.2
SDST	5.29E+03	1.1
MCS instrument	4.98E+03	1.0
ONC instrument	2.48E+03	0.5

Table 4
MRO bioburden estimates for top 5 hardware items not exempt by B&B analysis (stable case)

Item description by subsystem	B&B Adjusted bioburden	% Total requirement
HiRISE instrument	2.4E+05	48.3
Gussets	1.3E+04	2.6
Helium tank	1.02E+04	2.0
Mid deck	7.4E+03	1.5
Aft deck	1.7E+03	0.3

best (mean) values. Although NPR 8020.12C is silent on this subject, PP-approved Pre-launch reports for many Mars landers have been based on this approach. The entry heating was minimized by an entry due to orbital decay (minimum velocity). The orbiter mass was also minimized (with the propellant mass predicted at the end of the nominal science mission). This minimum mass also corresponds to a smaller heating rate. Finally, the most likely stable orientation for the stable entry case provides the least heating and the most components delivered to the surface. The heat fluxes at the stagnation point are believed to be very accurate, within the accuracy of well-established computer codes. The spatial distributions of the heat fluxes are only approximate within standard practice for the problem. However, CFD was used to verify and correct the approximation. When exposure of an object to the aeroflow was unclear or insufficient database existed, the heating was assumed to be zero. Avionics boxes (modules) were assumed to be randomly tumbling. Thus the heating was variable in time, which reduced its magnitude on any specific surface. The multinode code for detailed thermal analysis of the modules is also very accurate. It was used to verify the ablation model. The lumped mass model used for the electronics assemblies after the enclosure was removed underestimated heating because the area which would be exposed to the heating flux and the area available for thermal re-radiation were intentionally underestimated. In addition, no heat flux was applied until after the enclosure was completely ablated away. This approach neglected expected heating due to hot flow from partial enclosure burn-through at the edges and/or corners of the modules. The weakest point of the B&B analysis was probably the breakup analysis. By intent, the separation of orbiter components was delayed until the latest reasonable predicted time during entry. This was certainly conservative for the temperature attained by these components. However, the overall trajectory and heating of the bulk of the orbiter depend on the area presented to the flow and the mass (heat rate $\sim$m/A). Since the mass and area were decremented as the orbiter lost components, the conservatism for the bulk of the orbiter of a late separation of a component depends on whether m/A was larger or smaller after the separation. In most cases the heating rate difference was small and operated only for the limited duration of the separation time uncertainty. Unfortunately a sensitivity study for this issue was far beyond the resources available. Nevertheless, at most a small non-conservative error seems possible. The likely conclusion (unproven) is that the B&B analysis is very conservative because of all of its determinate conservative details.

The B&B analysis could be used to estimate the burden delivered to Mars by a mission that failed and entered the atmosphere in a non-nominal manner. This capability would be valuable in compliance with the PP requirements for the PP End of Mission Report. Specifically, it could have been applied to the Mars Climate Orbiter.

Acknowledgements

The work described in this report was carried out jointly by the Jet Propulsion Laboratory, California Institute of Technology and by Lockheed Martin Space Systems Company (LMSSC), Denver, CO, under a contract with NASA. Many others performed the detailed work summarized by the authors. At the Jet Propulsion Laboratory, the construction and maintenance of the PPEL was accomplished by Stephen Beverburg and Fabian Morales. W. Willcockson, S. Linch, M. Johnson, J. Bomba, K. Oakman, N. Tice, W. Kast, K. Piester, and M. Jouppi of LMSSC are responsible for the breakup and burn-up analysis.[31] The authors wish also to thank Wayne Schubert (JPL) for willing travel to other locations to obtain assay samples and for expert assays. Finally, Benton Clark (LMSSC) provided the technical and moral foundation of this effort at LMSSC.

[31] The details of the approach have been documented by LMSSC in an LMSSC internal report, Mars Reconnaissance Orbiter Planetary Protection Breakup and Burn-up Report, MRO-02-0127, DRD SE006-I-011b, Rev. B, June 2004.

References

NASA. Standard Procedures for the Microbiological Examination of Space Hardware, NHB 5340.1B, Rev. B, NASA HQ, Washington, DC, February 1980.

NASA. Planetary Protection Provisions for Robotic Extraterrestrial Missions, NASA Procedural Requirements NPR 8020.12C, NASA HQ, Washington, DC, April 2005.

Schubert, W., et al. Viability of bacterial spores exposed to hydrazine. J. Adv. Space Res., doi:10.1016/j.asr.2007.07.031.